JOURNAL OF VIROLOGY, May 2009, p. 4068–4080 Vol. 83, No. 9
0022-538X/09/$08.00+0 doi:10.1128/JVI.02486-08
Copyright © 2009, American Society for Microbiology. All Rights Reserved.

Major Coexisting Human Immunodeficiency Virus Type 1 *env* Gene Subpopulations in the Peripheral Blood Are Produced by Cells with Similar Turnover Rates and Show Little Evidence of Genetic Compartmentalization▽

William L. Ince,[1] Patrick R. Harrington,[2] Gretja L. Schnell,[2] Milloni Patel-Chhabra,[2] Christina L. Burch,[3] Prema Menezes,[4] Richard W. Price,[5] Joseph J. Eron, Jr.,[4] and Ronald I. Swanstrom[1,2,4]*

Curriculum in Genetics and Molecular Biology,[1] Department of Microbiology and Immunology,[2] Department of Biology,[3] and UNC Center for AIDS Research,[4] University of North Carolina, Chapel Hill, North Carolina 27599 and Department of Neurology, University of California, San Francisco, California 94143[5]

Received 3 December 2008/Accepted 3 February 2009

A distinctive feature of chronic human immunodeficiency virus type 1 (HIV-1) infection is the presence of multiple coexisting genetic variants, or subpopulations, that comprise the HIV-1 population detected in the peripheral blood. Analysis of HIV-1 RNA decay dynamics during the initiation of highly active antiretroviral therapy (HAART) has been a valuable tool for modeling the life span of infected cells that produce the bulk HIV-1 population. However, different HIV-1 target cells may have different turnover rates, and it is not clear whether the bulk HIV-1 RNA decay rate actually represents a composite of the decay rates of viral subpopulations compartmentalized in different cellular subsets with different life spans. Using heteroduplex tracking assays targeting the highly variable V3 or V4-V5 regions of the HIV-1 *env* gene in eight subjects, we found that all detectable coexisting HIV-1 variants in the peripheral blood generally decayed at similar rates during the initiation of HAART, suggesting that all of the variants were produced by cells with similar life spans. Furthermore, single genome amplification and coreceptor phenotyping revealed that in two subjects coexisting HIV-1 variants with distinct CXCR4 or CCR5 coreceptor phenotypes decayed with similar rates. Also, in nine additional subjects, recombination and a lack of genetic compartmentalization between X4 and R5 variants were observed, suggesting an overlap in host cell range. Our results suggest that the HIV-1 *env* subpopulations detectable in the peripheral blood are produced by cells with similar life spans and are not genetically isolated within particular cell types.

Infection with human immunodeficiency virus type 1 (HIV-1) is typically established by one or a few variants that give rise to an initially homogeneous viral population (12, 19, 38, 45). As infection progresses into the chronic phase, sequence diversification occurs throughout the viral genome, most dramatically in the envelope gene (*env*), as a result of selection of humoral and cytotoxic T-lymphocyte immune escape mutations (6, 20, 44, 74, 97). Sequence diversity in the *env* gene is clustered in variable regions, termed V1 through V5, that encode surface loops in the Env protein that are important targets of the host antibody response (20). Diversification of *env* results in the presence of multiple, coexisting *env* variants in the peripheral blood that continually evolve during the course of infection (31, 41).

Typically, the HIV-1 population early after infection uses CCR5 as the coreceptor (R5) (38, 93, 99, 101), and variants that can use CXCR4 (X4) arise later in the disease course in approximately one-half of individuals infected with subtype B virus (10, 42). A major determinant of coreceptor use is found in the V3 loop, and sequence evolution in this region is often linked to the virus's ability to use CXCR4 (17, 36, 54). After the emergence of X4 virus, *env* genes encoding both CCR5 and CXCR4 tropism can coexist for extended periods of time, maintaining a diverse V3 population (10, 54, 85). Variation in R5 Env proteins can also influence the ability of a virus to utilize various levels of CD4 and CCR5 found on different cell types, such as macrophages and T cells (23, 25, 64, 67, 89, 95).

Distinct biological characteristics encoded by different *env* variants, such as coreceptor use, cellular tropism, and sensitivity to immune pressure, may drive, or result from, HIV-1 compartmentalization. Genetic compartmentalization of HIV-1 variants has been well documented in anatomical compartments, such as the spleen (9, 18, 24), central nervous system (7, 29, 30, 43, 56, 73), and genital tract (13, 39, 60, 65, 70), and in different cellular compartments, such as monocyte/macrophage and $CD4^+$ T cells (21, 47). Divergent coreceptor tropism in particular may lead to compartmentalization of virus in different cellular subsets. For example, both naïve and memory T lymphocytes express CXCR4 but differentially express CCR5 and have been shown to harbor unequal proportions of CXCR4- and CCR5-tropic viral variants that are concordant with their distinct coreceptor expression patterns (3, 91).

While genetic compartmentalization of HIV-1 between anatomically or cellularly segregated sequences has been extensively explored, evidence is limited as to the extent to which the coexisting *env* subpopulations circulating in the peripheral blood represent virus emanating from compartmentalized populations replicating independently of each other and in differ-

* Corresponding author. Mailing address: Lineberger Comprehensive Cancer Center, University of North Carolina at Chapel Hill, CB #7295, Chapel Hill, NC 27599-7295. Phone: (919) 966 5710. Fax: (919) 966 8212. E-mail: risunc@med.unc.edu.

▽ Published ahead of print on 11 February 2009.

ent cellular subsets. Although this question is challenging to address in the context of an infected individual, one approach stems from the examination of the rate of decay of HIV-1 RNA during the initiation of highly active antiretroviral therapy (HAART). Effective HAART prevents new rounds of HIV-1 infection, but cells already infected by HIV-1 continue to produce virus, and therefore the rate of viral RNA decay during effective HAART reflects the life span of the HIV-1-producing cells. This strategy was initially used by Ho et al. and Wei et al. (34, 96) to characterize the turnover rate of HIV-1-infected cells. These and subsequent studies (4, 49, 62, 63) suggested that the average life span of infected cells that produce 99% or more of the bulk HIV-1 population in the peripheral blood is short, with a half-life of 1 to 2 days, presumably reflecting the life span of activated T cells, whereas cells producing 1% or less of the population have a half-life measured in weeks, illustrated by a biphasic decay curve. However, the bulk HIV-1 RNA decay rate of the first phase may oversimplify the dynamics of the underlying viral genetic subpopulations because this rate may represent an average without accounting for possible moderate differences between decay rates of coexisting variants, as might be the case for variants infecting cellular subsets in different stages of maturation or activation (22, 59, 100). Based on this model, two or more coexisting viral populations with the same rates of decay during HAART could be presumed to be produced by the same cellular subset or, at minimum, two or more subsets with the same turnover rate. Conversely, the observation of different rates of decay would suggest that different cellular subsets are contributing toward a complex mixture of compartmentalized viral subpopulations.

In this study we characterized the decay rates of coexisting HIV-1 *env* variants in the peripheral blood of eight subjects initiating HAART. In two of these subjects, who possessed both CCR5- and CXCR4-tropic Env variants, we analyzed the decay rates of each phenotypically divergent *env* subpopulation. Furthermore, in an additional nine subjects, we characterized the degree of recombination between the R5 and X4 subpopulations and the degree to which each subpopulation was genetically compartmentalized. We found that all detectible HIV-1 *env* variants in the peripheral blood, regardless of coreceptor tropism phenotype, decayed with similar rates during the initiation of HAART. In addition, we provide evidence of recombination and a lack of compartmentalization between coexisting X4 and R5 subpopulations, consistent with the overlap in their target host-cell populations. Our findings suggest that the detectable HIV-1 *env* variants that coexist in the peripheral blood are produced by cells with similar life spans and, by this measure, are not compartmentalized in particular cell types.

MATERIALS AND METHODS

Study subjects and sampling. Blood plasma samples used for the variant decay analysis were obtained from subjects initiating HAART who were recruited either through a previously described study carried out at the University of California, San Francisco (subjects 4015, 4021, 4022, 4030, and 5005) (87) or at the University of North Carolina, Chapel Hill (subjects 101, 106, 108, and 109), specifically for this study. Sampling of blood plasma was carried out on the day of treatment initiation and at 1- to 7-day intervals posttreatment initiation; the median time between samplings for all subjects was 3 days.

Additional blood plasma samples used for the analysis of recombination and compartmentalization in populations with mixed coreceptor use were excess tissue obtained from the baseline blood draw of subjects participating in the virology substudy of a ritonavir efficacy trial described previously (8) (subjects 1314, 1077, and 1551) or from baseline blood draws of subjects entering AIDS Clinical Trial Group 359 described elsewhere (subjects 432, 135, 139, 411, 413, and 310) (27). In all cases, written, informed consent was obtained and all protocols were subject to approval by the Institutional Review Board.

HTA and decay analysis. Viral RNA was extracted from virus particles pelleted from 1 ml of blood plasma (25,000 × *g* for 1.5 h) using a QiaAMP Viral RNA Kit (Qiagen, Chatsworth, CA). Two 5-μl aliquots of the 60-μl eluate were amplified in parallel using a OneStep RT-PCR kit (Qiagen, Chatsworth, CA). The PCR thermocycling procedures, the primers used to amplify the V3 and V4-V5 regions, and the heteroduplex tracking assays (HTAs) have been previously described (14, 31, 54). Briefly, PCR products were annealed to a radiolabeled probe to generate heteroduplexes, which were then separated in a polyacrylamide gel. Gel-separated heteroduplexes were visualized by autoradiography and quantitated on a Storm 840 phosphorimager using the ImageQuant software (Molecular Dynamics/GE, Pittsburgh, PA). The HTA was modified for this study by using a biotin-radiolabeled probe to facilitate isolation and sequencing of HTA bands, as described elsewhere (79). All samples were analyzed in duplicate to verify sampling reproducibility. Samples and time points that could not be reproducibly sampled were excluded from the analysis. Viral RNA loads (VLs) of individual variants were calculated as a product of the total viral RNA load and the fractional abundance of each variant. Variant half-lives were calculated using the time points between which VL was declining.

Single genome amplification (SGA). Viral RNA was extracted as described above. RNA was reverse transcribed using a Superscript III Reverse Transcriptase System (Invitrogen, CA) and oligo(dT). A region of the HIV-1 genome encompassing *env* through 3′ U3 was amplified using a limiting dilution, seminested PCR according to a method initially described by Simmonds et al. (82) and Edmonson and Mullins (16) and then modified by Palmer et al. (61) and Salazar-Gonzalez et al. (76). Primers and thermocycling procedures for amplification and sequencing were used as previously described in Keele et al. (38) but modified by replacing the downstream *env* amplification primer set with a primer that captures the U3, the sequence of which is 5′-AAGCACTCAAGGCAAGC TTTATTG-3′.

Coreceptor tropism analysis. Coreceptor phenotype was predicted based on V3 sequences of extracted HTA bands and SGA amplicons using a position-specific scoring matrix (PSSM) generated using a training set of V3 sequences from envelopes with known coreceptor phenotypes on indicator cells expressing CD4 and either CXCR4 or CCR5 (36). PSSM was implemented through the web portal http://ubik.microbiol.washington.edu/computing/pssm/.

Phenotypic analysis was carried out as previously described by Kirchherr et al. (40) but with modifications. Briefly, a cytomegalovirus (CMV) promoter containing a 3′ tag matching the 5′ SGA primer binding site was linked to *env* SGA amplicons using overlapping PCR. For the CMV-*env* linking PCR, the 5′ primer sequence is specific for the start of the CMV promoter (5′-AGTAATCAATTA CGGGGTCATTAGTTCAT-3′), and the downstream primer (5′-TGGGTGGC TCTGAAAAGAGCCTTTGGGCTGCTGGCTCAGCTCGTCTCATTCTTT C-3′) is specific for a sequence just 3′ of the end of *env* and contains a histone (H1e) mRNA 3′ stem-loop tag (underlined) for increased transcript stability. CMV-*env* amplicons were cotransfected with the pNL4-3.Luc.R$^-$E$^-$ plasmid, obtained from the NIH AIDS Research and Reference Reagent Program (32), to generate a pseudotyped, single-cycle luciferase reporter virus. The coreceptor phenotype of pseudotyped virus was assessed on U87.CD4 indicator cell lines, expressing either CXCR4 or CCR5, obtained from the NIH AIDS Research and Reference Reagent Program (2).

Compartmentalization and recombination analysis. All sequence alignments were generated using the program MAFFT (multiple alignment using fast Fourier transform) (37). Maximum-likelihood phylogenies were generated in PhyML using the HKY85 substitution rate model with the following parameters: use of four substitution rate categories and estimations of the transition/transversion rate ratio, proportion of invariant sites, and the gamma distribution parameter (26). A version of the Slatkin-Maddison (SM) test for gene flow was implemented using HyPhy (69, 83), and measures of K_{ST}^* were obtained using the program DnaSP (75). K_{ST}^* is calculated as described by Hudson, Boos, and Kaplan (35). Briefly, $K_{ST}^* = 1 - (K_S^*/K_T)$, where K_S^* is the weighted average of the log of the pairwise differences within each of the two potentially compartmentalized subpopulations, and K_T is the average number of pairwise differences between sequences, irrespective of their grouping. For both SM and K_{ST}^* tests, comparison of the observed result to the distribution of 1,000 random permutations of the data was used to obtain a *P* value. Recombination between X4 and R5 variants was detected in sequence alignments using the bootscan/RECSCAN analysis implemented in the Recombination Detection Program 3 (50, 78).

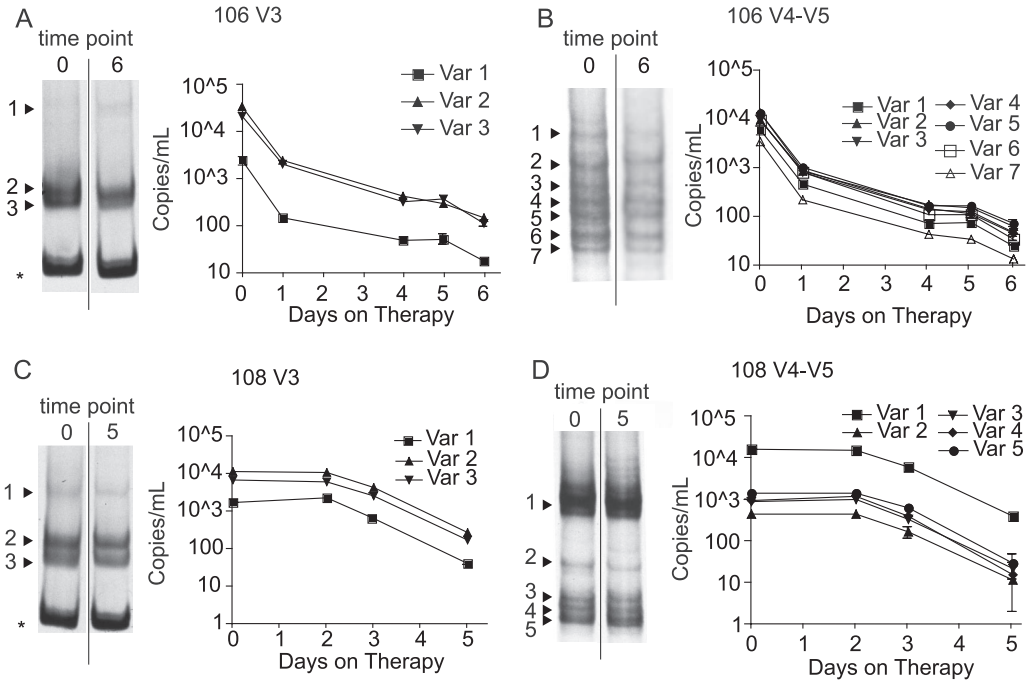

FIG. 1. HTA and variant decay analysis of V3 and V4-V5 envelope regions for subjects 106 (A and B) and 108 (C and D). Left panels depict HTA gel lanes for the first and last time points. Numbered arrows designate reproducible HTA variants. Asterisks indicate single-stranded probe bands. Right panels are plots of the VLs for individual variants (Var) at each time point sampled. Data points and error bars are the means and ranges, respectively, for two replicates. In subject 108, a decline in VL was not seen until after the second sampling time point; therefore, the decay rate was calculated from the second time point in this subject.

Bootscanning was carried out using a 200-bp window with a 20-bp step, and trees were constructed using the Jukes-Cantor model with 1,000 bootstrap replicates.

Nucleotide sequence accession numbers. Sequences determined in this study have been deposited in the GenBank database under accession numbers FJ798320 to FJ798580.

RESULTS

Decay rates do not vary between detectable *env* variants that coexist in the peripheral blood. We examined the decay rates of V4-V5 or V3 *env* variants in chronically infected subjects initiating HAART to characterize the life span of infected cells that produce coexisting genetic variants in the peripheral blood. Blood plasma samples from eight subjects were drawn every 1 to 7 days after the initiation of therapy, with a median interval of 3 days, for up to 3 weeks or over a 1- to 2-$\log_{10}$ drop in total VL. All subjects in this study achieved suppression of VL to below detectable levels. RNA was extracted from the plasma samples and then amplified by reverse transcription-PCR to generate amplicons of the variable regions V4-V5 or V3, which were then subjected to HTAs to resolve the coex-

TABLE 1. Subject characteristics and virus decay rates

Subject no.	No. of variants by HTA in the indicated region		Starting VL ($\log_{10}$)	CD4 count[g]	Log_{10} VL decrease	$t_{1/2}$ of bulk VL (days)[a]	% Least variant[b]	Max difference (fold) in $t_{1/2}$ (region)[c]
	V3	V4-V5						
101[d]	NA[e]	2	4.5	201	1.9	2.30	19	1.09 (V4-V5)
106	3	7	4.7	421	2.3	0.90[f]	5	1.14 (V3)
108	3	5	4.3	158	1.6	0.76	2	1.16 (V4-V5)
109[d]	2	4	4.9	23	2.1	1.09	11	1.24 (V4-V5)
4015	NA	2	5.1	NA	1.4	2.14	9	1.73
4021	NA	9	5.0	NA	1.0	1.20	2	2.0
4022	NA	4	4.6	NA	1.9	2.09	3	1.58
5005	NA	4	5.3	NA	1.5	2.27	2	1.60

[a] $t_{1/2}$, half-life.
[b] Percent relative abundance of the least abundant variant detected.
[c] Maximum (Max) difference (n-fold) in the half-life between any two variants.
[d] Subjects with mixed tropic virus populations.
[e] NA, data not available.
[f] Calculated using the first and last time points.
[g] CD4 count, no. of $CD4^+$ T cells/microliter of blood.

isting sequence variants. The relative abundance of V4-V5 or V3 variants, potentially comprising as little as 1 to 3% of the total population, was measured by phosphorimaging analysis of HTA bands (71, 79). Duplicate reverse transcription-PCRs were analyzed to ensure sampling reproducibility; the ability to analyze duplicate samples to validate the quality of sampling is a key feature of the HTA strategy as the HTA pattern of two identical, complex populations will appear different if they are not adequately sampled (33); however, the HTA pattern represents only variants whose sequence differences cause a shift in migration rate. While much of the diversity in these highly variable regions of the genome is captured using this technique, in this work we are testing the hypothesis that these HTA variants are markers of potentially compartmentalized populations.

The decay curves of V4-V5 and V3 HTA variants from two representative subjects are depicted Fig. 1. The $\log_{10}$ magnitude of the VL drop, the half-life (days) of the bulk VL, and the maximum differences in half-life for the *env* variants detected in each subject are shown in Table 1. In all but one subject, virus decay appeared monophasic over the first 1- to 2-$\log_{10}$ decline in VL. In subject 106, the VL decay appeared more rapid between the first and second time points (days 0 and 1), with an apparent half-life of 0.28 days (based on a single time point), than the VL decline between the second and fifth time points, with an apparent half-life of 2.22 days (Fig. 1a). The median half-life of the bulk VL decay rate for these subjects was 1.7 days. The decay rates of either V3 or V4-V5 variants within each subject did not vary significantly; the median value for the greatest differences between any two variants within a subject was 1.6-fold and did not exceed 2-fold within any subject, likely within the margin of error of this assay. The minor variation in decay rates of variants did not correlate with their relative abundance (Table 1). Thus, for variants comprising as little as 2% of the detected population and representing the first phase of decay, we conclude the following: (i) variants are not compartmentalized in anatomical locations or cellular compartments that are differentially targeted by antiviral activity; (ii) the life spans of potentially different, virus-producing cellular subsets do not differ to a significant degree for those cells producing the major variants of *env*; and (iii) variants are not otherwise compartmentalized in a manner that differentially affects their rates of decay.

Decay rates do not differ between X4 and R5 variants in the first phase of decay. The ability of a virus to use CXCR4 efficiently may allow infection of a different subset of target cells and hence may result in compartmentalization of X4 and R5 variants in cell types that differentially express these coreceptors, such as memory and naïve T-cell subsets (5). Many X4 variants retain the ability to enter cells using CCR5 (i.e., dual-tropic) although it is not clear this ability is utilized in vivo (48, 98). Furthermore, naïve and memory T-cell subsets have been shown to be preferentially infected by CXCR4 or CCR5 variants, respectively (3, 91).

We identified two subjects from the analysis described above who had coexisting CXCR4- and CCR5-tropic populations, which allowed us to determine the relative rates of decay of X4 and R5 variants specifically. Coreceptor usage was assessed by first using PSSM, followed by phenotypic analysis of the encoded Env protein in a pseudotyped virus entry assay, for a subset of sequences. One subject (109) had a viral population with both X4 and R5 variants identified by PSSM and confirmed in an entry assay. In the other subject (101), distinct V3 variants failed to meet the cutoff value for a CXCR4 tropism designation by PSSM but exhibited strong CXCR4-tropic activity in the entry assay. In both of these subjects, X4 variants retained some ability to use CCR5.

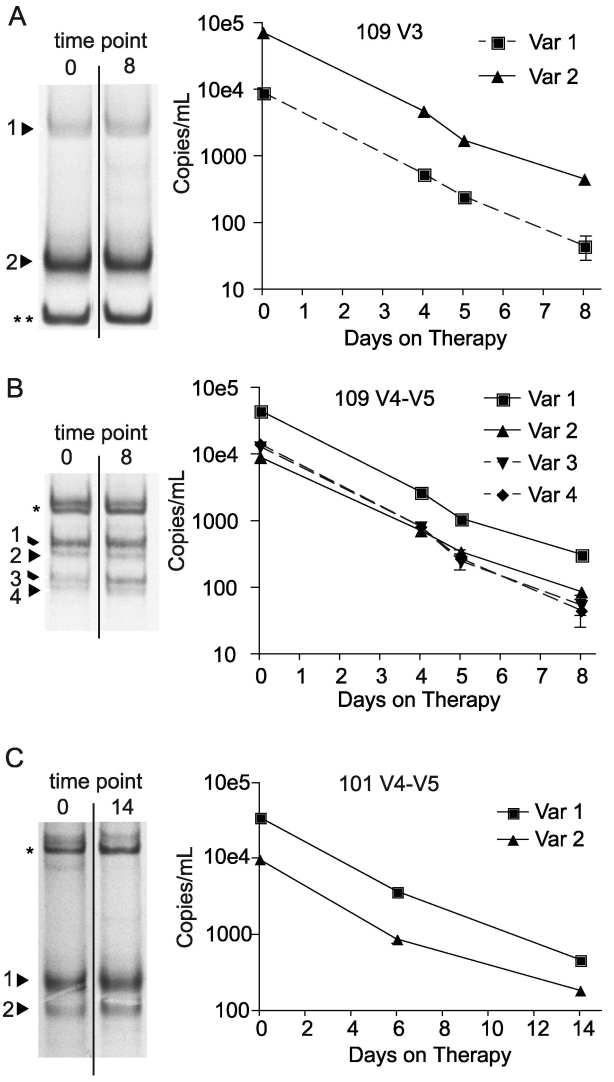

FIG. 2. HTA variant decay analysis of V3 and V4-V5 envelope regions for subjects 109 (A and B) and 101 (C) (V4-V5 only). Left panels depict HTA gel lanes for the first and last time points. Numbered arrows designate reproducible HTA variants. Single and double asterisks indicate single-stranded and double-stranded probe bands, respectively. Right panels are plots of the VLs for individual variants (Var) at each time point sampled. Data points and error bars are the means and ranges, respectively, for two replicates. Dashed lines indicate V3 and V4-V5 HTA variants linked to X4 usage.

HTA analysis of the V3 and V4-V5 regions of *env* of virus from subject 109 revealed two and four HTA variants, respectively (Fig. 2A and B). Recovery and sequencing of HTA bands, along with SGA and phylogenetic and phenotypic analysis of full-length *env* genes from the first time point, allowed us to link *env* sequences and their coreceptor usage phenotypes

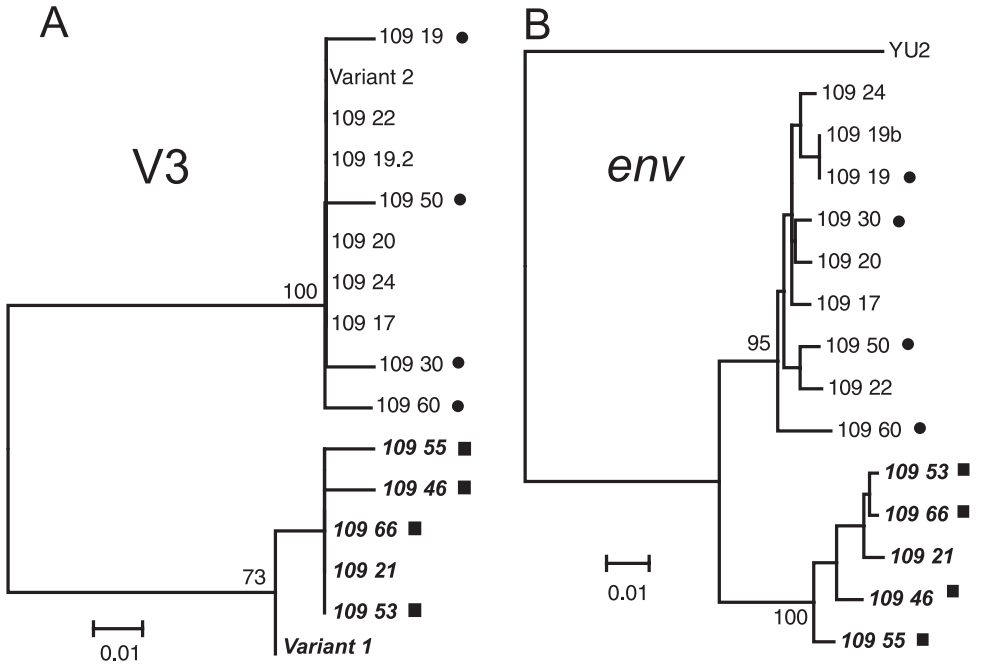

FIG. 3. Maximum-likelihood phylogenies of the V3 region (A) and full-length *env* (B) for subject 109. Node labels represent bootstrap values using 100 replicates. Italicized, bolded tip labels indicate *env* variants predicted to be X4 by PSSM. Circles indicate an entry assay R5 phenotype; squares indicate an entry assay X4 phenotype. The V3 tree was rooted at the midpoint. The *env* tree was rooted using the *env* sequence of the molecular clone YU2. V3 HTA variant sequences 1 and 2 correspond to variants in Fig. 2A.

to the specific V3 and V4-V5 HTA bands for this subject. For example, X4 and R5 V3 variants formed distinct phylogenetic lineages that were each represented by one of the two HTA variants (Fig. 3A), and V4-V5 HTA variants were linked to X4 V3 sequences by the presence of a deletion in each variable loop (data not shown). The full-length *env* sequences also formed distinct phylogenetic lineages according to V3 genotype and coreceptor phenotype (Fig. 3B). The decay of X4- and R5-linked V3 and V4-V5 HTA variants is depicted in Fig. 2A and B, respectively. The total VL decayed with a half-life of 2.3 days, and over the course of a 2-$\log_{10}$ drop in VL, there was no significant difference in the decay rates of HTA variants relative to each other in subject 109 (Fig. 2A and B; Table 1).

HTA analysis of virus from subject 101 revealed two variants in the V4-V5 region that decayed with similar rates (Fig. 2C and Table 1). However, we were not able to amplify the V3 region from this subject, presumably as a result of subsequently identified V3 primer binding site mismatches in this viral population. In an alternative approach taken for this subject, SGA was carried out on each time point in order to assess the change in the relative proportions of all SGA-amplified *env* variants as VL declined. *env* sequences that exhibited strong X4 usage in the entry assay clustered together in a phylogenetic tree, as did their V3 sequences, indicating linkage to coreceptor use (Fig. 4). While not meeting the threshold value for X4 usage according to PSSM, these V3 variants had distinctly higher PSSM values and were more positively charged relative to the rest of the population. V4-V5 genotypes were only weakly linked to tropism (data not shown). Weak X4 entry activity was detected in some envelopes whose sequences were intermingled with those of exclusively R5 envelopes (Fig. 4A) although the biological significance of this low-level X4 activity is unclear.

The decay rate of the total VL for subject 101 was a half-life of 2.3 days, and over the course of a 2-$\log_{10}$ drop in VL, there was no significant difference in the decay rates of V4-V5 HTA variants relative to each other (Fig. 2C and Table 1). In addition, we did not detect a significant change in the proportion of *env* sequence variants, sampled by SGA, that clustered with phenotypically identified X4 or R5 variants at the two time points following initiation of therapy. X4 variants constituted 26% of the amplicons in the first time point and 20% in the third time point ($P = 0.7$) (Fig. 4A). That we did not detect differential decay of X4 versus R5 variants in subjects 101 or 109 leads us to conclude that either (i) the bulk of the tropism variants are not compartmentalized in different cellular subsets, or (ii) while tropism variants may be compartmentalized in different cellular subsets, these infected cells have similar life spans when productively infected. Furthermore, any differential effects that X4 or R5 infection may have on the life span of the infected cell or any differences in susceptibility of these tropic variants to antiviral inhibition are not apparent in these data.

CXCR4- and CCR5-tropic variants exhibit limited genetic compartmentalization in the peripheral blood. We next examined the potential genetic compartmentalization of coexisting R5 and X4 variants using an alternative approach. For this analysis, we included the entry samples of the two subjects identified above (101 and 109) and an additional nine subjects, obtained from studies described in the Materials and Methods section, with coexisting X4 and R5 subpopulations identified

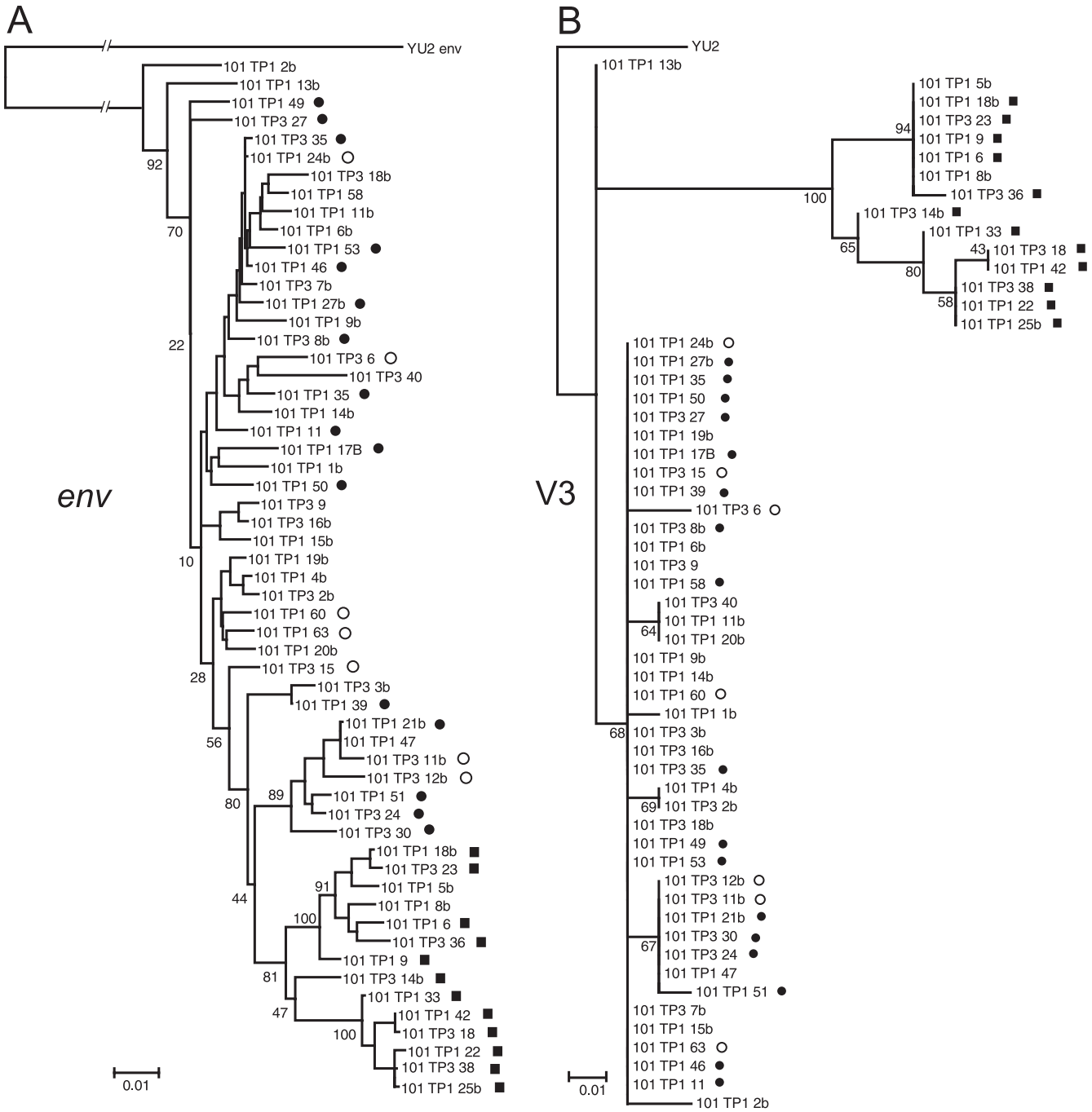

FIG. 4. Maximum-likelihood phylogenies of *env* (A) and V3 (B) sequences from day 0 (TP1) and day 14 (TP3) for subject 101. Node labels represent bootstrap values from 100 replicates. Trees were rooted using the molecular clone YU2. Closed circles indicate an entry assay R5 phenotype, squares indicate an entry assay X4 phenotype, and open circles indicate dual-tropic envelopes with weak X4 usage in an entry assay.

by PSSM analysis of V3 sequences. Using SGA, which eliminates confounding recombination during PCR, we generated amplicons containing *env*, *nef*, and the U3 region of the viral genome and carried out PSSM and phenotypic analysis on a representative subset of *env* variants from each subject. Phenotypic analysis was consistent with the result of the PSSM analysis for every amplicon tested in all but subject 101, as described above. CXCR4-tropic variants from all but two subjects in this study (138 and 411) also exhibited CCR5-tropic activity in the reporter assay but will be referred to as X4 variants. In many subjects, phylogenetic analysis of *env* sequences showed a deep branch point between the R5 sequences and a monophyletic group (i.e., a group that has descended from a single ancestral virus) of X4 sequences, suggesting that the outgrowth of X4 variants derives from a clonal event. Representative examples of phylogenies of se-

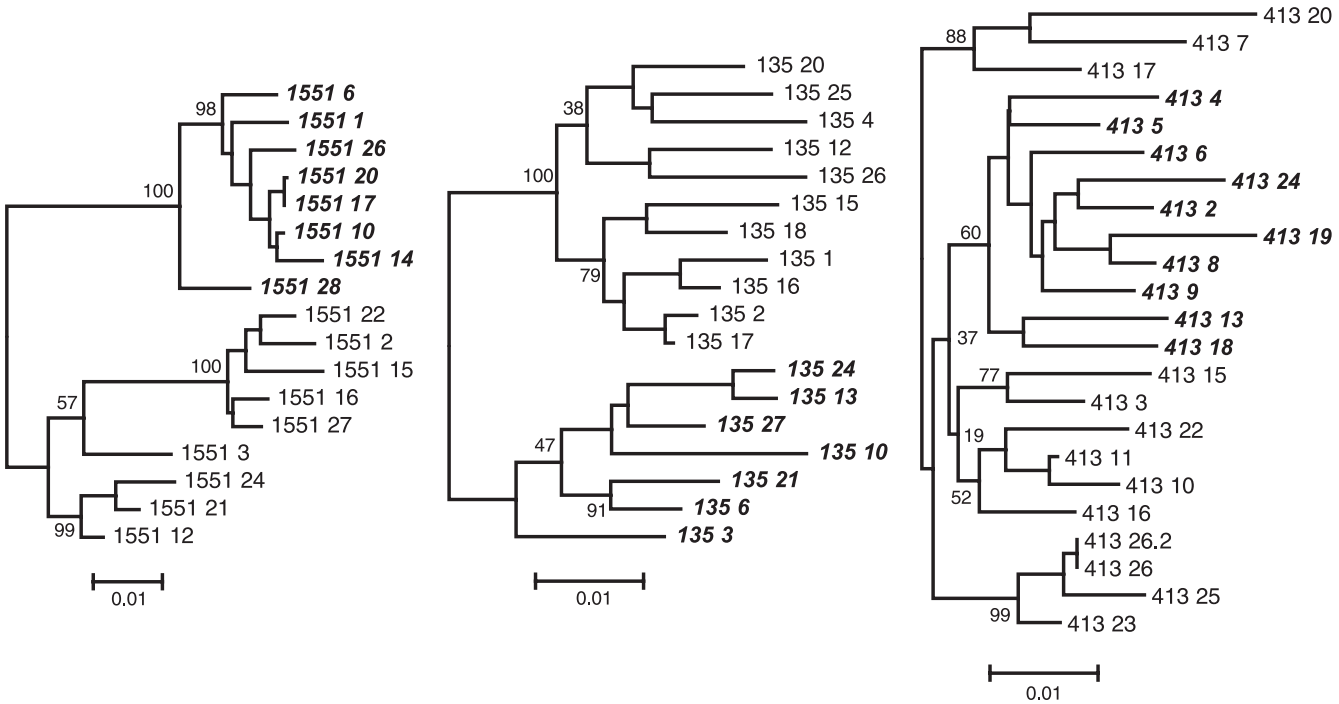

FIG. 5. Maximum-likelihood phylogenies of sequences encompassing *env* (starting at V1), *nef*, and U3 from three representative subjects (1551, 135, and 413) with distinct X4/dual and R5 populations. Node labels represent bootstrap values from 100 replicates. Italicized, bolded tip labels indicate *env* variants predicted to be X4 by PSSM and confirmed in an entry assay.

quences encompassing V1 of *env* through the 3′ U3 from three subjects are depicted in Fig. 5.

If these X4 and R5 variants exist in distinct compartments with no migration of viruses between compartments, then the independent evolution of these virus subpopulations will produce a number of evolutionary signatures in regions of the genome outside of V3. We looked for these signatures using two methods applied to sequences from three regions of the genome: the V4-V5 region of *env*, the gp41 region of *env*, and the U3 region of the long terminal repeat. First, we used the SM test (83) to investigate whether independent evolution of X4 and R5 variants in distinct compartments had produced similar phylogenetic patterns in all genome regions. Essentially, our use of the SM test examines the expectation that X4 viruses should form a monophyletic group, regardless of the genome region used to build the tree, if this group is compartmentalized. Second, we used a distance-based metric, K_{ST}* (see Materials and Methods) (34, 74, 89), to investigate whether independent evolution of X4 and R5 variants was occurring in distinct compartments and producing genetic differentiation between the compartments in regions outside of V3. The K_{ST}* statistic is a measure of whether the genetic distance (number of nucleotide differences) between the X4 and R5 subpopulations is significantly greater than the genetic distance among viruses within the X4 or R5 subpopulations. Gene flow between compartments would erode both of these signatures of independent evolution, and gene flow is expected to have the strongest impact on genomic regions that are most distant from V3, due to the increased likelihood of recombination.

Observed SM and K_{ST} values were compared to the distribution of 1,000 random permutations of branches or sequences to determine the level of significance of separation. Because X4 and R5 subgroups were essentially defined by their V3 genotypes, which in most subjects were monophyletic groups with highly similar genotypes, recombination events were inferred when the sequences of the regions analyzed did not cluster according to their linked V3 genotype, indicated by migration events in the SM analysis. However, a lack of compartmentalization can result in increased sequence homogeneity in regions distal to V3, and detection of recombination between X4 and R5 sequences in these regions is possible only in cases where there remain strong phylogenetic signals that result in a well-supported tree.

The analysis revealed statistical support, by both K_{ST} and SM measures, for compartmentalization of two genetic populations defined by coreceptor use for markers proximal to V3, such as V4-V5 (Fig. 6). This would be expected as mutations closer to the population-defining V3 sequence would likely persist in linkage disequilibrium for a longer period of time after the outgrowth of the X4 V3 mutations, especially if they are functionally linked to V3. However, in most subjects, SM migration events between the R5 and X4 populations were increased in regions more distal to V3, such as U3 (Fig. 6A), indicating that these populations were replicating at least part of the time in a shared cell type, providing the opportunity for recombination. Representative examples of detected recombination between X4 and R5 sequences and the predicted location of breakpoints, in these cases outside of gp120, are illustrated in Fig. 7. This result is consistent with previous observations of recombination between X4 and R5 viruses made using different methods (51, 77, 92). We also observed

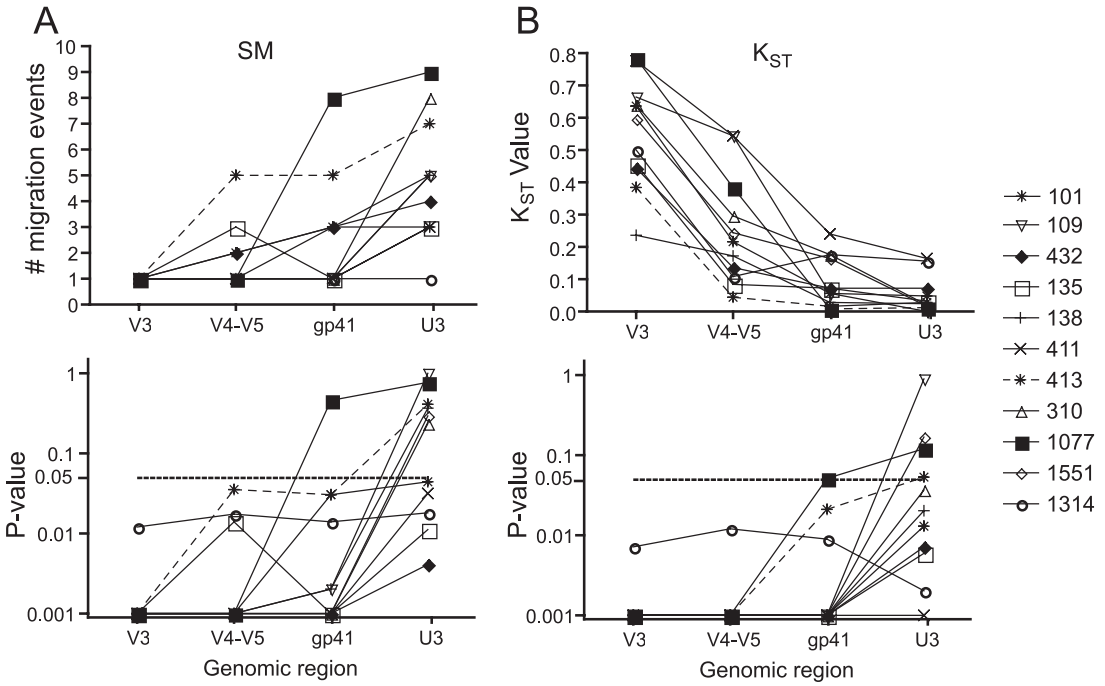

FIG. 6. Analysis of compartmentalization of four genomic regions between X4 and R5 variants. (A) SM test for branch migration events between X4 and R5 sequences (top) and corresponding *P* values (bottom) for support of compartmentalization for each region as determined in the SM test. (B) K_{ST}* values (top) and corresponding *P* values (bottom) for support of compartmentalization between X4 and R5 variants for each genome region as determined by the K_{ST}* test. Dashed line indicates a *P* value of 0.05.

decreasing values of genetic differentiation between X4 and R5 groups, as measured by $K_{ST,}$ for regions farther from V3 (Fig. 6b). However, in several subjects (135, 411, 432, and 1314) a compartmentalization signal in the U3 region remained statistically significant, if decreased, by both measures (Fig. 6, bottom panels). Taken together, these results show that while X4 and R5 *env* variants are genetically distinct, in many of our subjects there is little evidence of genetic compartmentalization between X4 and R5 variants in regions outside of *env*, such as in the U3.

DISCUSSION

There are several reasons to hypothesize that variants that appear in the blood are potentially compartmentalized. Previous studies have demonstrated compartmentalization of HIV-1 variants between different anatomical compartments, such as the central nervous system, genital tract, and different lymphoid tissues (13, 15, 24, 28, 39, 43, 70, 73, 77, 81, 90), as well as tissue microenvironments (24). The gut-associated lymphoid tissue, in particular, represents a major source of active replication of potentially compartmentalized CCR5-tropic virus populations (1, 68, 90, 94). It is possible that virus spatially compartmentalized in these anatomical sites may be represented as distinct variants in the peripheral blood. Because the initiation of HAART abruptly blocks new rounds of HIV-1 infection, presumably without impacting viral RNA production from cells already infected, different decay rates of compartmentalized variants following suppression of viral replication should reflect different life spans of the cells from which they are emerging. Viral populations compartmentalized in either cell types or tissues that experience differential drug exposure may also decay at different rates if viral replication continues at some level in the presence of a suboptimal drug concentration. However, our observation that all detectable HIV-1 genetic variants declined at comparable rates suggests that the vast majority of the coexisting HIV-1 subpopulations in the peripheral blood are not compartmentalized either in cell types with different life spans or in cells or tissues with various degrees of antiretroviral drug bioavailability.

Our use of the HTA allowed for relatively sensitive detection of variants potentially comprising as little as 1 to 3% of the population (33, 79). However, one important limitation of this study is the sensitivity for detection of minority viral populations below this 1% threshold, which may be produced by cells with different life spans. Such viral populations almost certainly exist, based on the biphasic decay kinetics of the bulk HIV-1 RNA load during HAART (4, 49, 62). It has been hypothesized that the second phase of decay of the bulk HIV-1 RNA load represents virus produced by cells with a longer life span, presumably cells of the monocyte lineage. Compartmentalization of viral DNA populations between $CD4^+$ T cells and monocytes has been reported (21, 47, 102), and assuming that monocytes have longer half-lives relative to activated $CD4^+$ T cells, variants compartmentalized in these different cell types would be expected to exhibit different rates of decay during HAART (11, 34, 62, 96). However, the proportion of variants compartmentalized in productively infected monocytes may be

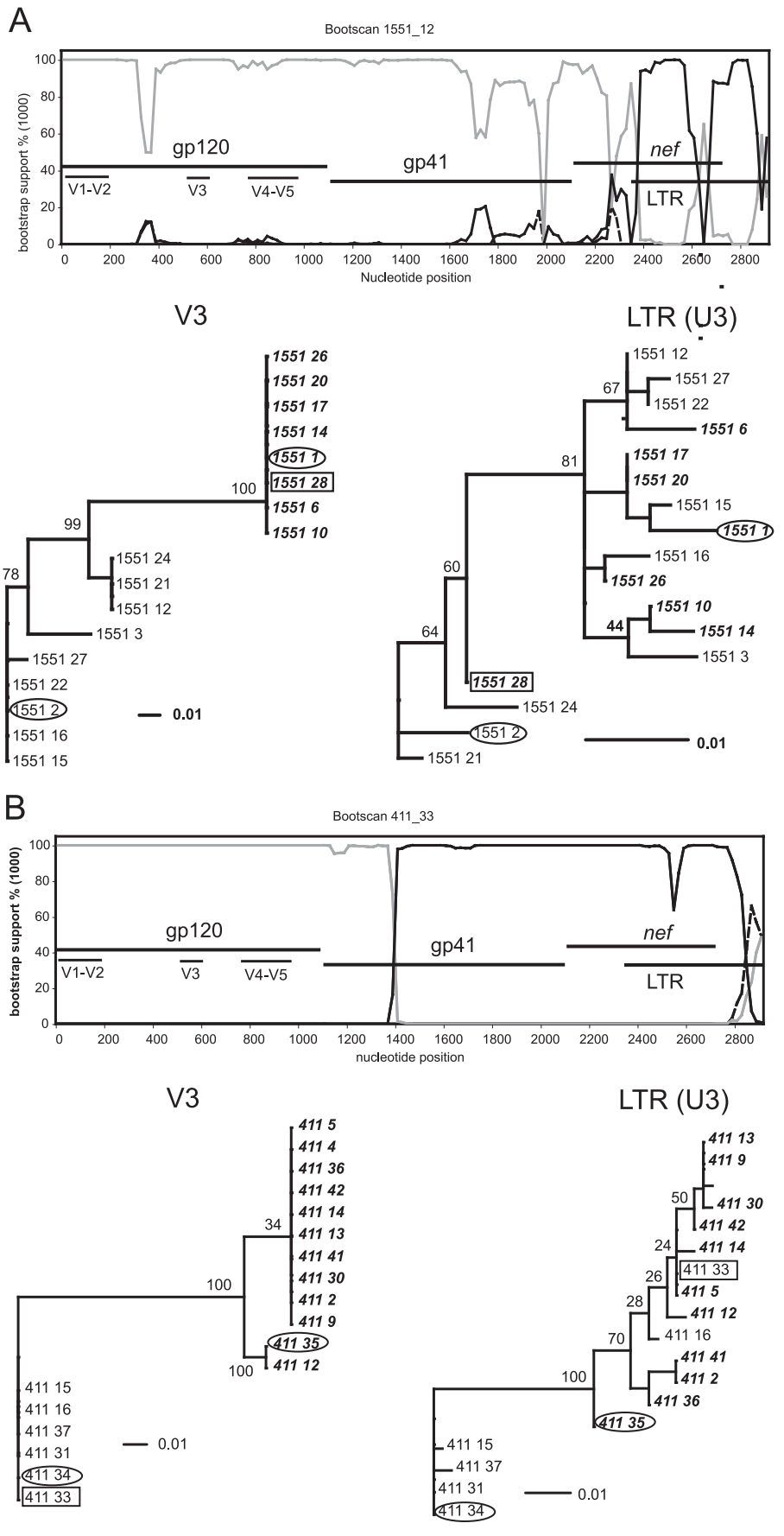
A
Bootscan 1551_12
bootstrap support % (1000)
Nucleotide position
gp120
gp41
nef
LTR
V1-V2
V3
V4-V5
V3
LTR (U3)
1551 26
1551 20
1551 17
1551 14
1551 1
1551 28
1551 6
1551 10
1551 24
1551 21
1551 12
1551 3
1551 27
1551 22
1551 2
1551 16
1551 15
0.01
1551 12
1551 27
1551 22
1551 6
1551 17
1551 20
1551 15
1551 1
1551 16
1551 26
1551 10
1551 14
1551 3
1551 28
1551 24
1551 2
1551 21
0.01
B
Bootscan 411_33
bootstrap support % (1000)
nucleotide position
gp120
gp41
nef
LTR
V1-V2
V3
V4-V5
V3
LTR (U3)
411 5
411 4
411 36
411 42
411 14
411 13
411 41
411 30
411 2
411 9
411 35
411 12
411 15
411 16
411 37
411 31
411 34
411 33
0.01
411 13
411 9
411 30
411 42
411 14
411 33
411 5
411 12
411 16
411 41
411 2
411 36
411 35
411 15
411 37
411 31
411 34
0.01

too small to be detected in our assay (62, 63), and monocytes may not be productively infected and only produce virus upon entry into tissue and differentiation (72, 84). Furthermore, the decay characteristics of HIV-1 upon initiation of therapy that includes an integrase inhibitor suggest that much of the second phase of decay observed in conventional therapy represents cells that are slowly undergoing integration and that the proportion of productively infected, long-lived cells is smaller than previously thought (53, 80). Another limitation of this study is that it depends on the assumption that compartmentalized subpopulations can be distinguished by their *env* genotypes and, in particular, genotypes that can be resolved by HTA. However, in addition to its function in determining host cell tropism, the extreme genetic complexity of *env* within infected individuals makes it a highly sensitive target for the detection of coexisting viral subpopulations, and any other genomic region that may drive HIV-1 compartmentalization would likely be linked to distinct *env* variants as a result of founder effects, genetic isolation, or compartment-specific evolution. Furthermore, any compartmentalized variants would have likely diverged enough to be resolved by HTA analysis (30). Thus, we can conservatively conclude that the lack of genetic compartmentalization and the differential decay rates observed in this study apply to the bulk of the HIV-1 population in the peripheral blood that represents primarily the first phase of viral RNA decay during HAART.

Another potential opportunity for cellular compartmentalization is between naïve and memory $CD4^+$ T cells. While naïve and memory T cells express similar levels of CXCR4, CCR5 is expressed only in memory cells (5, 46, 55). Previous studies have found a wide range of preferential infection by, and potential compartmentalization of, X4 and R5 variants in these cell types in a manner consistent with their coreceptor expression patterns (3, 57, 91). If X4 and R5 variants are compartmentalized in these two cell types to a significant degree, then similarity in decay rates would indicate that the life spans of infected naïve and memory cells are similar when they become activated and produce virus. It is thought that the bulk of viral replication occurs in activated $CD4^+$ memory T cells (34, 49, 62, 86, 88, 100), in which case any potential compartmentalization of R5 and X4 variants observed in resting memory and naïve cells may represent only a small fraction of the total population. Also, activated and previously activated T cells express both CCR5 and CXCR4 (5, 55, 58), providing a potential source of mixing of R5 and X4 variants. There is evidence to suggest that the pool of cells supporting the bulk of virus replication is not homogeneous in its susceptibility to infection by X4 and R5 variants (22) and that X4 and R5 variants may be differentially affected by antiretroviral therapy (22, 66). However, we found no difference in the decay rates of X4 and R5 variants upon initiation of therapy, and the decay rates of these variants are within the range reported in other studies for the first phase of decay, presumably reflecting the life spans of the activated memory cells supporting ~99% of the virus population (34, 49, 62, 63, 96). This finding is consistent with a model where virus is emerging from a homogeneous pool of cells that is sufficiently susceptible to infection by both X4 and R5 variants to account for most of the production of these variants found in the periphery. This is also further supported by the finding of a lack of genetic compartmentalization between X4 and R5 populations in both subjects 101 and 109 for regions outside of *env*, indicating some overlap of target cell types. However, the lack of data indicating differential decay rates of variants does not allow a definitive conclusion to be drawn regarding the half-lives of infected cells in different cellular subsets until the degree of cellular compartmentalization of X4 and R5 variants can be more fully and directly accounted for in studies of this type.

The divergent X4 and R5 lineages indicate some degree of genetic compartmentalization between these variants. This could be due to physical isolation in different cell types or to genetic linkage selected across *env* for the ability to use different coreceptors. However, we detected an overall lack of compartmentalization and evidence of recombination between these populations in sequence regions increasingly distal of 3′ of V3, suggesting the potential for sequence mixing between R5 and X4 variants in a coinfected cell (Fig. 6 and 7). This observation is consistent with previous reports that have identified X4/R5 recombinants both within *env* and between *env* and other regions of the genome (51, 77, 92). However, our use of the single genome amplification approach avoided the possibility of recombination during PCR, which may have created artificial recombinants in some previous studies. These data support the conclusion that while X4 and R5 variants may preferentially replicate in distinct cellular compartments, they are not genetically isolated and must with some frequency infect the same cell types. Still, the deep branch points in the phylogenetic trees suggest that the initial outgrowth of X4 variants is from a monoclonal genotype.

This study found little evidence for differential decay and compartmentalization of *env* variants comprising the bulk of the virus in the peripheral blood, even in the case of divergent coreceptor phenotypes, indicating that HAART is equally effective on all the detectible variants making up the bulk virus in the peripheral blood. However, new technologies are becoming available that will allow sampling to below 1% (52), and the application of these technologies may yet reveal minor populations that exhibit differential rates of decay upon initiation of therapy.

FIG. 7. Representative examples of recombination between X4 and R5 variants in subjects 1551 (A) and 411 (B) Top panels show bootscanning plots identifying recombination breakpoints. The horizontal axis indicates the nucleotide position in the putative recombinant (query sequence) and in the genomic regions mapped within the plot. The vertical axis is the percent bootstrap support (1,000 replicates) for clustering of the query sequence with either the R5 (gray) or X4 (black) putative parental sequences. Bottom panels show maximum-likelihood trees of V3 (left) and U3 (right) regions indicated in the bootscan plots. X4 variants are italicized and bolded. Recombinants are boxed and putative parents are circled. LTR, long terminal repeat.

ACKNOWLEDGMENTS

This work was supported by NIH grant R37-AI44667 to R.S.; an AmFAR award to P.H.; NIH training grant support to W.I. (T32-GM07092), G.S. (T32-AI07001), M.P.C. (T32-AI07419), and P.H. (T32-CA09156); the UNC Center For AIDS Research (NIH award P30-AI50410); and the UNC General Clinical Research Center.

We thank Dale Kempf from Abbott and the AIDS Clinical Trial Group 359 study team for making samples available for this study.

REFERENCES

1. **Arthos, J., C. Cicala, E. Martinelli, K. Macleod, D. Van Ryk, D. Wei, Z. Xiao, T. D. Veenstra, T. P. Conrad, R. A. Lempicki, S. McLaughlin, M. Pascuccio, R. Gopaul, J. McNally, C. C. Cruz, N. Censoplano, E. Chung, K. N. Reitano, S. Kottilil, D. J. Goode, and A. S. Fauci.** 2008. HIV-1 envelope protein binds to and signals through integrin $\alpha4\beta7$, the gut mucosal homing receptor for peripheral T cells. Nat. Immunol. **9:**301–309.
2. **Bjorndal, A., H. Deng, M. Jansson, J. R. Fiore, C. Colognesi, A. Karlsson, J. Albert, G. Scarlatti, D. R. Littman, and E. M. Fenyo.** 1997. Coreceptor usage of primary human immunodeficiency virus type 1 isolates varies according to biological phenotype. J. Virol. **71:**7478–7487.
3. **Blaak, H., A. B. van't Wout, M. Brouwer, B. Hooibrink, E. Hovenkamp, and H. Schuitemaker.** 2000. In vivo HIV-1 infection of $CD45RA^+$ $CD4^+$ T cells is established primarily by syncytium-inducing variants and correlates with the rate of $CD4^+$ T cell decline. Proc. Natl. Acad. Sci. USA **97:**1269–1274.
4. **Blankson, J. N., D. Finzi, T. C. Pierson, B. P. Sabundayo, K. Chadwick, J. B. Margolick, T. C. Quinn, and R. F. Siliciano.** 2000. Biphasic decay of latently infected CD4+ T cells in acute human immunodeficiency virus type 1 infection. J. Infect. Dis. **182:**1636–1642.
5. **Bleul, C. C., L. Wu, J. A. Hoxie, T. A. Springer, and C. R. Mackay.** 1997. The HIV coreceptors CXCR4 and CCR5 are differentially expressed and regulated on human T lymphocytes. Proc. Natl. Acad. Sci. USA **94:**1925–1930.
6. **Borrow, P., H. Lewicki, X. Wei, M. S. Horwitz, N. Peffer, H. Meyers, J. A. Nelson, J. E. Gairin, B. H. Hahn, M. B. Oldstone, and G. M. Shaw.** 1997. Antiviral pressure exerted by HIV-1-specific cytotoxic T lymphocytes (CTLs) during primary infection demonstrated by rapid selection of CTL escape virus. Nat. Med. **3:**205–211.
7. **Burkala, E. J., J. He, J. T. West, C. Wood, and C. K. Petito.** 2005. Compartmentalization of HIV-1 in the central nervous system: role of the choroid plexus. AIDS **19:**675–684.
8. **Cameron, D. W., M. Heath-Chiozzi, S. Danner, C. Cohen, S. Kravcik, C. Maurath, E. Sun, D. Henry, R. Rode, A. Potthoff, J. Leonard, et al.** 1998. Randomised placebo-controlled trial of ritonavir in advanced HIV-1 disease. Lancet **351:**543–549.
9. **Cheynier, R., S. Henrichwark, F. Hadida, E. Pelletier, E. Oksenhendler, B. Autran, and S. Wain-Hobson.** 1995. Clonal expansion of T cells and HIV genotypes in microdissected splenic white pulps indicates viral replication in situ and infiltration of HIV-specific cytotoxic T lymphocytes. Adv. Exp. Med. Biol. **374:**173–182.
10. **Connor, R. I., K. E. Sheridan, D. Ceradini, S. Choe, and N. R. Landau.** 1997. Change in coreceptor use coreceptor use correlates with disease progression in HIV-1-infected individuals. J. Exp. Med. **185:**621–628.
11. **Crowe, S., T. Zhu, and W. A. Muller.** 2003. The contribution of monocyte infection and trafficking to viral persistence, and maintenance of the viral reservoir in HIV infection. J. Leukoc. Biol. **74:**635–641.
12. **Delwart, E., M. Magierowska, M. Royz, B. Foley, L. Peddada, R. Smith, C. Heldebrant, A. Conrad, and M. Busch.** 2002. Homogeneous quasispecies in 16 out of 17 individuals during very early HIV-1 primary infection. AIDS **16:**189–195.
13. **Delwart, E. L., J. I. Mullins, P. Gupta, G. H. Learn, Jr., M. Holodniy, D. Katzenstein, B. D. Walker, and M. K. Singh.** 1998. Human immunodeficiency virus type 1 populations in blood and semen. J. Virol. **72:**617–623.
14. **Delwart, E. L., H. W. Sheppard, B. D. Walker, J. Goudsmit, and J. I. Mullins.** 1994. Human immunodeficiency virus type 1 evolution in vivo tracked by DNA heteroduplex mobility assays. J. Virol. **68:**6672–6683.
15. **Diem, K., D. C. Nickle, A. Motoshige, A. Fox, S. Ross, J. I. Mullins, L. Corey, R. W. Coombs, and J. N. Krieger.** 2008. Male genital tract compartmentalization of human immunodeficiency virus type 1 (HIV). AIDS Res. Hum. Retrovir. **24:**561–571.
16. **Edmonson, P. F., and J. I. Mullins.** 1992. Efficient amplification of HIV half-genomes from tissue DNA. Nucleic Acids Res. **20:**4933.
17. **Fouchier, R. A., M. Groenink, N. A. Kootstra, M. Tersmette, H. G. Huisman, F. Miedema, and H. Schuitemaker.** 1992. Phenotype-associated sequence variation in the third variable domain of the human immunodeficiency virus type 1 gp120 molecule. J. Virol. **66:**3183–3187.
18. **Frost, S. D., M. J. Dumaurier, S. Wain-Hobson, and A. J. Brown.** 2001. Genetic drift and within-host metapopulation dynamics of HIV-1 infection. Proc. Natl. Acad. Sci. USA **98:**6975–6980.
19. **Frost, S. D., Y. Liu, S. L. Pond, C. Chappey, T. Wrin, C. J. Petropoulos, S. J. Little, and D. D. Richman.** 2005. Characterization of human immunodeficiency virus type 1 (HIV-1) envelope variation and neutralizing antibody responses during transmission of HIV-1 subtype B. J. Virol. **79:**6523–6527.
20. **Frost, S. D., T. Wrin, D. M. Smith, S. L. Kosakovsky Pond, Y. Liu, E. Paxinos, C. Chappey, J. Galovich, J. Beauchaine, C. J. Petropoulos, S. J. Little, and D. D. Richman.** 2005. Neutralizing antibody responses drive the evolution of human immunodeficiency virus type 1 envelope during recent HIV infection. Proc. Natl. Acad. Sci. USA **102:**18514–18519.
21. **Fulcher, J. A., Y. Hwangbo, R. Zioni, D. Nickle, X. Lin, L. Heath, J. I. Mullins, L. Corey, and T. Zhu.** 2004. Compartmentalization of human immunodeficiency virus type 1 between blood monocytes and $CD4^+$ T cells during infection. J. Virol. **78:**7883–7893.
22. **Gondois-Rey, F., A. Biancotto, M. A. Fernandez, L. Bettendroffer, J. Blazkova, K. Trejbalova, M. Pion, and I. Hirsch.** 2006. R5 variants of human immunodeficiency virus type 1 preferentially infect $CD62L^-$ $CD4^+$ T cells and are potentially resistant to nucleoside reverse transcriptase inhibitors. J. Virol. **80:**854–865.
23. **Gorry, P. R., J. Taylor, G. H. Holm, A. Mehle, T. Morgan, M. Cayabyab, M. Farzan, H. Wang, J. E. Bell, K. Kunstman, J. P. Moore, S. M. Wolinsky, and D. Gabuzda.** 2002. Increased CCR5 affinity and reduced CCR5/CD4 dependence of a neurovirulent primary human immunodeficiency virus type 1 isolate. J. Virol. **76:**6277–6292.
24. **Gratton, S., R. Cheynier, M. J. Dumaurier, E. Oksenhendler, and S. Wain-Hobson.** 2000. Highly restricted spread of HIV-1 and multiply infected cells within splenic germinal centers. Proc. Natl. Acad. Sci. USA **97:**14566–14571.
25. **Gray, L., J. Sterjovski, M. Churchill, P. Ellery, N. Nasr, S. R. Lewin, S. M. Crowe, S. L. Wesselingh, A. L. Cunningham, and P. R. Gorry.** 2005. Uncoupling coreceptor usage of human immunodeficiency virus type 1 (HIV-1) from macrophage tropism reveals biological properties of CCR5-restricted HIV-1 isolates from patients with acquired immunodeficiency syndrome. Virology **337:**384–398.
26. **Guindon, S., and O. Gascuel.** 2003. A simple, fast, and accurate algorithm to estimate large phylogenies by maximum likelihood. Syst. Biol. **52:**696–704.
27. **Gulick, R. M., X. J. Hu, S. A. Fiscus, C. V. Fletcher, R. Haubrich, H. Cheng, E. Acosta, S. W. Lagakos, R. Swanstrom, W. Freimuth, S. Snyder, C. Mills, M. Fischl, C. Pettinelli, and D. Katzenstein.** 2000. Randomized study of saquinavir with ritonavir or nelfinavir together with delavirdine, adefovir, or both in human immunodeficiency virus-infected adults with virologic failure on indinavir: AIDS Clinical Trials Group Study 359. J. Infect. Dis. **182:**1375–1384.
28. **Haddad, D. N., C. Birch, T. Middleton, D. E. Dwyer, A. L. Cunningham, and N. K. Saksena.** 2000. Evidence for late stage compartmentalization of HIV-1 resistance mutations between lymph node and peripheral blood mononuclear cells. Aids **14:**2273–2281.
29. **Harrington, P. R., M. J. Connell, R. B. Meeker, P. R. Johnson, and R. Swanstrom.** 2007. Dynamics of simian immunodeficiency virus populations in blood and cerebrospinal fluid over the full course of infection. J. Infect. Dis. **196:**1058–1067.
30. **Harrington, P. R., D. W. Haas, K. Ritola, and R. Swanstrom.** 2005. Compartmentalized human immunodeficiency virus type 1 present in cerebrospinal fluid is produced by short-lived cells. J. Virol. **79:**7959–7966.
31. **Harrington, P. R., J. A. Nelson, K. M. Kitrinos, and R. Swanstrom.** 2007. Independent evolution of human immunodeficiency virus type 1 *env* V1/V2 and V4/V5 hypervariable regions during chronic infection. J. Virol. **81:**5413–5417.
32. **He, J., S. Choe, R. Walker, P. Di Marzio, D. O. Morgan, and N. R. Landau.** 1995. Human immunodeficiency virus type 1 viral protein R (Vpr) arrests cells in the G2 phase of the cell cycle by inhibiting p34cdc2 activity. J. Virol. **69:**6705–6711.
33. **Henderson, G. J., N. G. Hoffman, L. H. Ping, S. A. Fiscus, I. F. Hoffman, K. M. Kitrinos, T. Banda, F. E. Martinson, P. N. Kazembe, D. A. Chilongozi, M. S. Cohen, and R. Swanstrom.** 2004. HIV-1 populations in blood and breast milk are similar. Virology **330:**295–303.
34. **Ho, D. D., A. U. Neumann, A. S. Perelson, W. Chen, J. M. Leonard, and M. Markowitz.** 1995. Rapid turnover of plasma virions and CD4 lymphocytes in HIV-1 infection. Nature **373:**123–126.
35. **Hudson, R. R., D. D. Boos, and N. L. Kaplan.** 1992. A statistical test for detecting geographic subdivision. Mol. Biol. Evol. **9:**138–151.
36. **Jensen, M. A., F. S. Li, A. B. van't Wout, D. C. Nickle, D. Shriner, H. X. He, S. McLaughlin, R. Shankarappa, J. B. Margolick, and J. I. Mullins.** 2003. Improved coreceptor usage prediction and genotypic monitoring of R5-to-X4 transition by motif analysis of human immunodeficiency virus type 1 *env* V3 loop sequences. J. Virol. **77:**13376–13388.
37. **Katoh, K., and H. Toh.** 2008. Recent developments in the MAFFT multiple sequence alignment program. Brief Bioinform. **9:**286–298.
38. **Keele, B. F., E. E. Giorgi, J. F. Salazar-Gonzalez, J. M. Decker, K. T. Pham, M. G. Salazar, C. Sun, T. Grayson, S. Wang, H. Li, X. Wei, C. Jiang, J. L. Kirchherr, F. Gao, J. A. Anderson, L. H. Ping, R. Swanstrom, G. D. Tomaras, W. A. Blattner, P. A. Goepfert, J. M. Kilby, M. S. Saag, E. L. Delwart, M. P. Busch, M. S. Cohen, D. C. Montefiori, B. F. Haynes, B. Gaschen, G. S. Athreya, H. Y. Lee, N. Wood, C. Seoighe, A. S. Perelson, T.**

Bhattacharya, B. T. Korber, B. H. Hahn, and G. M. Shaw. 2008. Identification and characterization of transmitted and early founder virus envelopes in primary HIV-1 infection. Proc. Natl. Acad. Sci. USA **105:**7552–7557.

39. **Kemal, K. S., B. Foley, H. Burger, K. Anastos, H. Minkoff, C. Kitchen, S. M. Philpott, W. Gao, E. Robison, S. Holman, C. Dehner, S. Beck, W. A. Meyer III, A. Landay, A. Kovacs, J. Bremer, and B. Weiser.** 2003. HIV-1 in genital tract and plasma of women: compartmentalization of viral sequences, coreceptor usage, and glycosylation. Proc. Natl. Acad. Sci. USA **100:**12972–12977.
40. **Kirchherr, J. L., X. Lu, W. Kasongo, V. Chalwe, L. Mwananyanda, R. M. Musonda, S. M. Xia, R. M. Scearce, H. X. Liao, D. C. Montefiori, B. F. Haynes, and F. Gao.** 2007. High throughput functional analysis of HIV-1 *env* genes without cloning. J. Virol. Methods **143:**104–111.
41. **Kitrinos, K. M., N. G. Hoffman, J. A. Nelson, and R. Swanstrom.** 2003. Turnover of env variable region 1 and 2 genotypes in subjects with late-stage human immunodeficiency virus type 1 infection. J. Virol. **77:**6811–6822.
42. **Koot, M., R. van Leeuwen, R. E. de Goede, I. P. Keet, S. Danner, J. K. Eeftinck Schattenkerk, P. Reiss, M. Tersmette, J. M. Lange, and H. Schuitemaker.** 1999. Conversion rate towards a syncytium-inducing (SI) phenotype during different stages of human immunodeficiency virus type 1 infection and prognostic value of SI phenotype for survival after AIDS diagnosis. J. Infect. Dis. **179:**254–258.
43. **Korber, B. T., K. J. Kunstman, B. K. Patterson, M. Furtado, M. M. McEvilly, R. Levy, and S. M. Wolinsky.** 1994. Genetic differences between blood- and brain-derived viral sequences from human immunodeficiency virus type 1-infected patients: evidence of conserved elements in the V3 region of the envelope protein of brain-derived sequences. J. Virol. **68:**7467–7481.
44. **Koup, R. A., J. T. Safrit, Y. Cao, C. A. Andrews, G. McLeod, W. Borkowsky, C. Farthing, and D. D. Ho.** 1994. Temporal association of cellular immune responses with the initial control of viremia in primary human immunodeficiency virus type 1 syndrome. J. Virol. **68:**4650–4655.
45. **Learn, G. H., D. Muthui, S. J. Brodie, T. Zhu, K. Diem, J. I. Mullins, and L. Corey.** 2002. Virus population homogenization following acute human immunodeficiency virus type 1 infection. J. Virol. **76:**11953–11959.
46. **Lee, B., M. Sharron, L. J. Montaner, D. Weissman, and R. W. Doms.** 1999. Quantification of CD4, CCR5, and CXCR4 levels on lymphocyte subsets, dendritic cells, and differentially conditioned monocyte-derived macrophages. Proc. Natl. Acad. Sci. USA **96:**5215–5220.
47. **Llewellyn, N., R. Zioni, H. Zhu, T. Andrus, Y. Xu, L. Corey, and T. Zhu.** 2006. Continued evolution of HIV-1 circulating in blood monocytes with antiretroviral therapy: genetic analysis of HIV-1 in monocytes and $CD4^+$ T cells of patients with discontinued therapy. J. Leukoc. Biol. **80:**1118–1126.
48. **Malkevitch, N., D. H. McDermott, Y. Yi, J. C. Grivel, D. Schols, E. De Clercq, P. M. Murphy, S. Glushakova, R. G. Collman, and L. Margolis.** 2001. Coreceptor choice and T cell depletion by R5, X4, and R5X4 HIV-1 variants in CCR5-deficient (CCR5Δ32) and normal human lymphoid tissue. Virology **281:**239–247.
49. **Markowitz, M., M. Louie, A. Hurley, E. Sun, M. Di Mascio, A. S. Perelson, and D. D. Ho.** 2003. A novel antiviral intervention results in more accurate assessment of human immunodeficiency virus type 1 replication dynamics and T-cell decay in vivo. J. Virol. **77:**5037–5038.
50. **Martin, D. P., D. Posada, K. A. Crandall, and C. Williamson.** 2005. A modified bootscan algorithm for automated identification of recombinant sequences and recombination breakpoints. AIDS Res. Hum. Retrovir. **21:**98–102.
51. **Mild, M., J. Esbjornsson, E. M. Fenyo, and P. Medstrand.** 2007. Frequent intrapatient recombination between human immunodeficiency virus type 1 R5 and X4 envelopes: implications for coreceptor switch. J. Virol. **81:**3369–3376.
52. **Mitsuya, Y., V. Varghese, C. Wang, T. F. Liu, S. P. Holmes, P. Jayakumar, B. Gharizadeh, M. Ronaghi, D. Klein, W. J. Fessel, and R. W. Shafer.** 2008. Minority human immunodeficiency virus type 1 variants in antiretroviral-naive persons with reverse transcriptase codon 215 revertant mutations. J. Virol. **82:**10747–10755.
53. **Murray, J. M., S. Emery, A. D. Kelleher, M. Law, J. Chen, D. J. Hazuda, B. Y. Nguyen, H. Teppler, and D. A. Cooper.** 2007. Antiretroviral therapy with the integrase inhibitor raltegravir alters decay kinetics of HIV, significantly reducing the second phase. AIDS **21:**2315–2321.
54. **Nelson, J. A., F. Baribaud, T. Edwards, and R. Swanstrom.** 2000. Patterns of changes in human immunodeficiency virus type 1 V3 sequence populations late in infection. J. Virol. **74:**8494–8501.
55. **Nicholson, J. K., S. W. Browning, R. L. Hengel, E. Lew, L. E. Gallagher, D. Rimland, and J. S. McDougal.** 2001. CCR5 and CXCR4 expression on memory and naive T cells in HIV-1 infection and response to highly active antiretroviral therapy. J. Acquir. Immune Defic. Syndr. **27:**105–115.
56. **Ohagen, A., A. Devitt, K. J. Kunstman, P. R. Gorry, P. P. Rose, B. Korber, J. Taylor, R. Levy, R. L. Murphy, S. M. Wolinsky, and D. Gabuzda.** 2003. Genetic and functional analysis of full-length human immunodeficiency virus type 1 *env* genes derived from brain and blood of patients with AIDS. J. Virol. **77:**12336–12345.
57. **Ostrowski, M. A., T. W. Chun, S. J. Justement, I. Motola, M. A. Spinelli, J. Adelsberger, L. A. Ehler, S. B. Mizell, C. W. Hallahan, and A. S. Fauci.** 1999. Both memory and $CD45RA^+/CD62L^+$ naive $CD4^+$ T cells are infected in human immunodeficiency virus type 1-infected individuals. J. Virol. **73:**6430–6435.
58. **Ostrowski, M. A., S. J. Justement, A. Catanzaro, C. A. Hallahan, L. A. Ehler, S. B. Mizell, P. N. Kumar, J. A. Mican, T. W. Chun, and A. S. Fauci.** 1998. Expression of chemokine receptors CXCR4 and CCR5 in HIV-1-infected and uninfected individuals. J. Immunol. **161:**3195–3201.
59. **Ostrowski, M. A., D. C. Krakauer, Y. Li, S. J. Justement, G. Learn, L. A. Ehler, S. K. Stanley, M. Nowak, and A. S. Fauci.** 1998. Effect of immune activation on the dynamics of human immunodeficiency virus replication and on the distribution of viral quasispecies. J. Virol. **72:**7772–7784.
60. **Overbaugh, J., R. J. Anderson, J. O. Ndinya-Achola, and J. K. Kreiss.** 1996. Distinct but related human immunodeficiency virus type 1 variant populations in genital secretions and blood. AIDS Res. Hum. Retrovir. **12:**107–115.
61. **Palmer, S., M. Kearney, F. Maldarelli, E. K. Halvas, C. J. Bixby, H. Bazmi, D. Rock, J. Falloon, R. T. Davey, Jr., R. L. Dewar, J. A. Metcalf, S. Hammer, J. W. Mellors, and J. M. Coffin.** 2005. Multiple, linked human immunodeficiency virus type 1 drug resistance mutations in treatment-experienced patients are missed by standard genotype analysis. J. Clin. Microbiol. **43:**406–413.
62. **Perelson, A. S., P. Essunger, Y. Cao, M. Vesanen, A. Hurley, K. Saksela, M. Markowitz, and D. D. Ho.** 1997. Decay characteristics of HIV-1-infected compartments during combination therapy. Nature **387:**188–191.
63. **Perelson, A. S., A. U. Neumann, M. Markowitz, J. M. Leonard, and D. D. Ho.** 1996. HIV-1 dynamics in vivo: virion clearance rate, infected cell life-span, and viral generation time. Science **271:**1582–1586.
64. **Peters, P. J., J. Bhattacharya, S. Hibbitts, M. T. Dittmar, G. Simmons, J. Bell, P. Simmonds, and P. R. Clapham.** 2004. Biological analysis of human immunodeficiency virus type 1 R5 envelopes amplified from brain and lymph node tissues of AIDS patients with neuropathology reveals two distinct tropism phenotypes and identifies envelopes in the brain that confer an enhanced tropism and fusigenicity for macrophages. J. Virol. **78:**6915–6926.
65. **Philpott, S., H. Burger, C. Tsoukas, B. Foley, K. Anastos, C. Kitchen, and B. Weiser.** 2005. Human immunodeficiency virus type 1 genomic RNA sequences in the female genital tract and blood: compartmentalization and intrapatient recombination. J. Virol. **79:**353–363.
66. **Philpott, S., B. Weiser, K. Anastos, C. M. Kitchen, E. Robison, W. A. Meyer, 3rd, H. S. Sacks, U. Mathur-Wagh, C. Brunner, and H. Burger.** 2001. Preferential suppression of CXCR4-specific strains of HIV-1 by antiviral therapy. J. Clin. Investig. **107:**431–438.
67. **Platt, E. J., K. Wehrly, S. E. Kuhmann, B. Chesebro, and D. Kabat.** 1998. Effects of CCR5 and CD4 cell surface concentrations on infections by macrophagetropic isolates of human immunodeficiency virus type 1. J. Virol. **72:**2855–2864.
68. **Poles, M. A., W. J. Boscardin, J. Elliott, P. Taing, M. M. Fuerst, I. McGowan, S. Brown, and P. A. Anton.** 2006. Lack of decay of HIV-1 in gut-associated lymphoid tissue reservoirs in maximally suppressed individuals. J. Acquir. Immune Defic. Syndr. **43:**65–68.
69. **Pond, S. L., S. D. Frost, and S. V. Muse.** 2005. HyPhy: hypothesis testing using phylogenies. Bioinformatics **21:**676–679.
70. **Poss, M., A. G. Rodrigo, J. J. Gosink, G. H. Learn, D. de Vange Panteleeff, H. L. Martin, Jr., J. Bwayo, J. K. Kreiss, and J. Overbaugh.** 1998. Evolution of envelope sequences from the genital tract and peripheral blood of women infected with clade A human immunodeficiency virus type 1. J. Virol. **72:**8240–8251.
71. **Resch, W., N. Parkin, E. L. Stuelke, T. Watkins, and R. Swanstrom.** 2001. A multiple-site-specific heteroduplex tracking assay as a tool for the study of viral population dynamics. Proc. Natl. Acad. Sci. USA **98:**176–181.
72. **Rich, E. A., I. S. Chen, J. A. Zack, M. L. Leonard, and W. A. O'Brien.** 1992. Increased susceptibility of differentiated mononuclear phagocytes to productive infection with human immunodeficiency virus-1 (HIV-1). J. Clin. Investig. **89:**176–183.
73. **Ritola, K., K. Robertson, S. A. Fiscus, C. Hall, and R. Swanstrom.** 2005. Increased human immunodeficiency virus type 1 (HIV-1) *env* compartmentalization in the presence of HIV-1-associated dementia. J. Virol. **79:**10830–10834.
74. **Ross, H. A., and A. G. Rodrigo.** 2002. Immune-mediated positive selection drives human immunodeficiency virus type 1 molecular variation and predicts disease duration. J. Virol. **76:**11715–11720.
75. **Rozas, J., and R. Rozas.** 1999. DnaSP version 3: an integrated program for molecular population genetics and molecular evolution analysis. Bioinformatics **15:**174–175.
76. **Salazar-Gonzalez, J. F., E. Bailes, K. T. Pham, M. G. Salazar, M. B. Guffey, B. F. Keele, C. A. Derdeyn, P. Farmer, E. Hunter, S. Allen, O. Manigart, J. Mulenga, J. A. Anderson, R. Swanstrom, B. F. Haynes, G. S. Athreya, B. T. Korber, P. M. Sharp, G. M. Shaw, and B. H. Hahn.** 2008. Deciphering

human immunodeficiency virus type 1 transmission and early envelope diversification by single-genome amplification and sequencing. J. Virol. **82:**3952–3970.

77. **Salemi, M., B. R. Burkhardt, R. R. Gray, G. Ghaffari, J. W. Sleasman, and M. M. Goodenow.** 2007. Phylodynamics of HIV-1 in lymphoid and non-lymphoid tissues reveals a central role for the thymus in emergence of CXCR4-using quasispecies. PLoS ONE **2:**e950.
78. **Salminen, M. O., J. K. Carr, D. S. Burke, and F. E. McCutchan.** 1995. Identification of breakpoints in intergenotypic recombinants of HIV type 1 by bootscanning. AIDS Res. Hum. Retrovir. **11:**1423–1425.
79. **Schnell, G., W. L. Ince, and R. Swanstrom.** 2008. Identification and recovery of minor HIV-1 variants using the heteroduplex tracking assay and biotinylated probes. Nucleic Acids Res. **36:**e146.
80. **Sedaghat, A. R., J. B. Dinoso, L. Shen, C. O. Wilke, and R. F. Siliciano.** 2008. Decay dynamics of HIV-1 depend on the inhibited stages of the viral life cycle. Proc. Natl. Acad. Sci. USA **105:**4832–4837.
81. **Shapshak, P., D. M. Segal, K. A. Crandall, R. K. Fujimura, B. T. Zhang, K. Q. Xin, K. Okuda, C. K. Petito, C. Eisdorfer, and K. Goodkin.** 1999. Independent evolution of HIV type 1 in different brain regions. AIDS Res. Hum. Retrovir. **15:**811–820.
82. **Simmonds, P., P. Balfe, C. A. Ludlam, J. O. Bishop, and A. J. Brown.** 1990. Analysis of sequence diversity in hypervariable regions of the external glycoprotein of human immunodeficiency virus type 1. J. Virol. **64:**5840–5850.
83. **Slatkin, M., and W. P. Maddison.** 1989. A cladistic measure of gene flow inferred from the phylogenies of alleles. Genetics **123:**603–613.
84. **Sonza, S., A. Maerz, N. Deacon, J. Meanger, J. Mills, and S. Crowe.** 1996. Human immunodeficiency virus type 1 replication is blocked prior to reverse transcription and integration in freshly isolated peripheral blood monocytes. J. Virol. **70:**3863–3869.
85. **Stalmeijer, E. H., R. P. Van Rij, B. Boeser-Nunnink, J. A. Visser, M. A. Naarding, D. Schols, and H. Schuitemaker.** 2004. In vivo evolution of X4 human immunodeficiency virus type 1 variants in the natural course of infection coincides with decreasing sensitivity to CXCR4 antagonists. J. Virol. **78:**2722–2728.
86. **Stanley, S. K., M. A. Ostrowski, J. S. Justement, K. Gantt, S. Hedayati, M. Mannix, K. Roche, D. J. Schwartzentruber, C. H. Fox, and A. S. Fauci.** 1996. Effect of immunization with a common recall antigen on viral expression in patients infected with human immunodeficiency virus type 1. N. Engl. J. Med. **334:**1222–1230.
87. **Staprans, S., N. Marlowe, D. Glidden, T. Novakovic-Agopian, R. M. Grant, M. Heyes, F. Aweeka, S. Deeks, and R. W. Price.** 1999. Time course of cerebrospinal fluid responses to antiretroviral therapy: evidence for variable compartmentalization of infection. AIDS **13:**1051–1061.
88. **Stevenson, M., T. L. Stanwick, M. P. Dempsey, and C. A. Lamonica.** 1990. HIV-1 replication is controlled at the level of T cell activation and proviral integration. EMBO J. **9:**1551–1560.
89. **Thomas, E. R., R. L. Dunfee, J. Stanton, D. Bogdan, J. Taylor, K. Kunstman, J. E. Bell, S. M. Wolinsky, and D. Gabuzda.** 2007. Macrophage entry mediated by HIV Envs from brain and lymphoid tissues is determined by the capacity to use low CD4 levels and overall efficiency of fusion. Virology **360:**105–119.
90. **van Marle, G., M. J. Gill, D. Kolodka, L. McManus, T. Grant, and D. L. Church.** 2007. Compartmentalization of the gut viral reservoir in HIV-1 infected patients. Retrovirology **4:**87.
91. **van Rij, R. P., H. Blaak, J. A. Visser, M. Brouwer, R. Rientsma, S. Broersen, A. M. de Roda Husman, and H. Schuitemaker.** 2000. Differential coreceptor expression allows for independent evolution of non-syncytium-inducing and syncytium-inducing HIV-1. J. Clin. Investig. **106:**1039–1052.
92. **van Rij, R. P., M. Worobey, J. A. Visser, and H. Schuitemaker.** 2003. Evolution of R5 and X4 human immunodeficiency virus type 1 *gag* sequences in vivo: evidence for recombination. Virology **314:**451–459.
93. **van't Wout, A. B., N. A. Kootstra, G. A. Mulder-Kampinga, N. Albrecht-van Lent, H. J. Scherpbier, J. Veenstra, K. Boer, R. A. Coutinho, F. Miedema, and H. Schuitemaker.** 1994. Macrophage-tropic variants initiate human immunodeficiency virus type 1 infection after sexual, parenteral, and vertical transmission. J. Clin. Investig. **94:**2060–2067.
94. **Veazey, R. S., M. DeMaria, L. V. Chalifoux, D. E. Shvetz, D. R. Pauley, H. L. Knight, M. Rosenzweig, R. P. Johnson, R. C. Desrosiers, and A. A. Lackner.** 1998. Gastrointestinal tract as a major site of $CD4^+$ T cell depletion and viral replication in SIV infection. Science **280:**427–431.
95. **Walter, B. L., K. Wehrly, R. Swanstrom, E. Platt, D. Kabat, and B. Chesebro.** 2005. Role of low CD4 levels in the influence of human immunodeficiency virus type 1 envelope V1 and V2 regions on entry and spread in macrophages. J. Virol. **79:**4828–4837.
96. **Wei, X., S. K. Ghosh, M. E. Taylor, V. A. Johnson, E. A. Emini, P. Deutsch, J. D. Lifson, S. Bonhoeffer, M. A. Nowak, B. H. Hahn, et al.** 1995. Viral dynamics in human immunodeficiency virus type 1 infection. Nature **373:**117–122.
97. **Wolinsky, S. M., B. T. Korber, A. U. Neumann, M. Daniels, K. J. Kunstman, A. J. Whetsell, M. R. Furtado, Y. Cao, D. D. Ho, and J. T. Safrit.** 1996. Adaptive evolution of human immunodeficiency virus-type 1 during the natural course of infection. Science **272:**537–542.
98. **Yi, Y., F. Shaheen, and R. G. Collman.** 2005. Preferential use of CXCR4 by R5X4 human immunodeficiency virus type 1 isolates for infection of primary lymphocytes. J. Virol. **79:**1480–1486.
99. **Zhang, L. Q., P. MacKenzie, A. Cleland, E. C. Holmes, A. J. Brown, and P. Simmonds.** 1993. Selection for specific sequences in the external envelope protein of human immunodeficiency virus type 1 upon primary infection. J. Virol. **67:**3345–3356.
100. **Zhang, Z., T. Schuler, M. Zupancic, S. Wietgrefe, K. A. Staskus, K. A. Reimann, T. A. Reinhart, M. Rogan, W. Cavert, C. J. Miller, R. S. Veazey, D. Notermans, S. Little, S. A. Danner, D. D. Richman, D. Havlir, J. Wong, H. L. Jordan, T. W. Schacker, P. Racz, K. Tenner-Racz, N. L. Letvin, S. Wolinsky, and A. T. Haase.** 1999. Sexual transmission and propagation of SIV and HIV in resting and activated $CD4^+$ T cells. Science **286:**1353–1357.
101. **Zhu, T., H. Mo, N. Wang, D. S. Nam, Y. Cao, R. A. Koup, and D. D. Ho.** 1993. Genotypic and phenotypic characterization of HIV-1 patients with primary infection. Science **261:**1179–1181.
102. **Zhu, T., D. Muthui, S. Holte, D. Nickle, F. Feng, S. Brodie, Y. Hwangbo, J. I. Mullins, and L. Corey.** 2002. Evidence for human immunodeficiency virus type 1 replication in vivo in $CD14^+$ monocytes and its potential role as a source of virus in patients on highly active antiretroviral therapy. J. Virol. **76:**707–716.